



Contents lists available at ScienceDirect

## Journal of Hand Surgery Global Online

journal homepage: [www.JHSGO.org](http://www.JHSGO.org)

## Original Research

# Histological Comparison of Porcine Small Intestine Submucosa and Bovine Type-I Collagen Conduit for Nerve Repair in a Rat Model



Rasa Zhukauskas, MD, \* Debbie Neubauer Fischer, MS, \* Curt Deister, PhD, \* Jennifer Faleris, MPM, \* Stefanie B. Marquez-Vilendrer, PhD, \* Deana Mercer, MD †

\* Axogen Corporation, Alachua, FL

† University of New Mexico, Albuquerque, NM

## ARTICLE INFO

**Article history:**

Received for publication May 2, 2023

Accepted in revised form July 15, 2023

Available online August 30, 2023

**Key words:**

Foamy cells

Foamy phagocytes

Macrophages

Peripheral nerve regeneration

Schwann cells

**Purpose:** After nerve injury, macrophages and Schwann cells remove axon and myelin debris. We hypothesized that nerves repaired with different conduit materials will result in varying levels of these cell populations, which impacts Wallerian degeneration and axonal regeneration.

**Methods:** We performed a unilateral sciatic nerve transection in 18 rats. The nerves were repaired with small intestine submucosa (SIS, n = 9) or isolated type-I collagen (CLC, n = 9) conduits. Rats were monitored for 4 weeks. Histology samples were obtained from the proximal nerve, mid-implant, and distal nerve regions. Samples were stained for total macrophages, M2 macrophages, foamy phagocytes, Schwann cells, vascular components, axon components, and collagen density.

**Results:** Distal nerve analyses showed higher populations of total macrophages and M2 macrophages in SIS-repaired nerves and higher density of foamy phagocytes in CLC-repaired nerves. Proximal nerve, mid-implant, and distal nerve analyses showed higher Schwann cell and vascular component densities in SIS-repaired nerves. Axon density was higher in the mid-implant region of SIS-repaired nerves. Collagen staining in the mid-implant was scant, but less collagen density was observed in SIS-repaired versus CLC-repaired nerves.

**Conclusions:** In the distal nerve, the following were observed: (1) lower total macrophages in CLC-repaired nerves, suggesting lower overall inflammation versus SIS-repaired nerves; (2) higher M2 macrophages in SIS-repaired versus CLC-repaired nerves, a driving factor for higher total macrophages and indicative of an inflammation resolution response in SIS-repaired nerves; and (3) a lower foamy phagocyte density in SIS-repaired nerves, suggesting earlier resolution of Wallerian degeneration versus CLC-repaired nerves. In the proximal nerve, mid-implant, and distal nerve, higher Schwann cell and vascular component densities were noted in SIS-repaired nerves. In the mid-implant, a higher axon component density and a lower collagen density of the SIS-repaired nerves versus CLC-repaired nerves were noted. These results indicate more robust nerve regeneration with less collagen deposition.

**Clinical relevance:** This *in vivo* study evaluated two common conduit materials that are used in peripheral nerve repair. Clinical outcomes of nerves repaired with conduits may be impacted by the response to different conduit materials. These nerve repair responses include Wallerian degeneration, nerve regeneration, and nerve scarring. This study evaluated Wallerian degeneration using total macrophages, M2 macrophages, and foamy phagocytes. Nerve regeneration was evaluated using Schwann cells and axons. Nerve scarring was evaluated using vascular and collagen density.

Copyright © 2023, THE AUTHORS. Published by Elsevier Inc. on behalf of The American Society for Surgery of the Hand. This is an open access article under the CC BY-NC-ND license (<http://creativecommons.org/licenses/by-nc-nd/4.0/>).

**Declaration of interests:** No benefits in any form have been received or will be received related directly to this article.

**Corresponding author:** Rasa Zhukauskas, MD, Axogen Corporation, 111 West Oak Ave., suite 500 Tampa, Alachua, FL 33602.

E-mail address: [rzhukauskas@axogeninc.com](mailto:rzhukauskas@axogeninc.com) (R. Zhukauskas).

<https://doi.org/10.1016/j.jhsg.2023.07.014>

2589-5141/Copyright © 2023, THE AUTHORS. Published by Elsevier Inc. on behalf of The American Society for Surgery of the Hand. This is an open access article under the CC BY-NC-ND license (<http://creativecommons.org/licenses/by-nc-nd/4.0/>).

After a nerve transection injury, surgical repair may be performed using a direct repair or a nerve reconstruction with autograft, allograft, or conduit. The selection of the nerve repair technique is highly dependent on the nerve gap size, where nerve gaps less than 5 mm can be repaired directly or reconstructed with a nerve conduit. Use of a nerve conduit may facilitate nerve alignment as the conduit acts as a coupling device and may

decrease tension, stabilize and align the coaptation, and contain the neurotropic milieu.<sup>1</sup> Commercially available nerve conduits comprise various synthetic and natural materials (e.g., porcine pericardium, porcine small intestine submucosa (SIS), isolated type-I collagen (CLC), chitosan, polyglycolic acid, and polyvinyl alcohol hydrogel).<sup>2</sup> Various material attributes have been investigated for nerve conduits including mechanical stability, degradation, handling, permeability, and biocompatibility.<sup>3</sup> The ideal nerve conduit should be biocompatible, exhibit an appropriate degradation rate, allow for oxygen and nutrient exchange while containing the neurotropic milieu, maintain mechanical stability throughout regeneration, and permit axonal outgrowth.<sup>3,4</sup> Furthermore, nerve conduits should not be detrimental to the natural Wallerian degeneration and nerve regeneration processes after neurotmetic injury.

Wallerian degeneration occurs in the peripheral nerve distal to the injury site. During early Wallerian degeneration, the myelinating Schwann cells stop producing myelin, de-differentiate into repair-type Schwann cells, upregulate gene expression for molecules that function in nerve degeneration and regeneration, and proliferate.<sup>5,6</sup> Simultaneously, macrophages are recruited to the injury site, which peaks approximately 7 days after injury.<sup>7–9</sup> In the distal nerve stump, the repair-type Schwann cells and macrophages remove axonal and myelin debris, which are barriers to axonal regeneration, within 14 days of injury.<sup>5–7,9,10</sup> Macrophages differentiate into either a proinflammatory M1 phenotype or an anti-inflammatory M2 phenotype, which further influences inflammation and nerve regeneration.<sup>8,11,12</sup> When macrophages ingest myelin during Wallerian degeneration, they become foamy phagocytes, which exhibit a notable presence of lipids within the cells.<sup>13,14</sup> Foamy phagocytes play a key role in the progression of Wallerian degeneration, and it is theorized that foamy phagocytes transport lipids (e.g., myelin) into the circulatory system for disposal.<sup>8,15</sup> The presence of these foamy phagocytes has not yet been investigated in peripheral nerves repaired with nerve conduits; however, the macrophage phenotype has been investigated.

A recently published *in vivo* nerve transection study evaluated the host response to implanted conduits in the proximal nerve stump through the distal region of the nerve conduit.<sup>16</sup> The study showed a higher M2:M1 response, more revascularization, and more fibroblast ingrowth through the mid-implant wall of SIS nerve conduits and more regenerated nerve cable density of the mid-implant region of SIS-repaired nerves versus CLC-repaired nerves at 4 weeks post-transection.<sup>16</sup> In this study, we evaluated the host response to implanted conduits in the proximal nerve, nerve conduit, and distal nerve stump. We hypothesized that more M2 macrophages and Schwann cells and fewer foamy phagocytes measured in the distal nerve stump provide an environment conducive to better axonal regeneration and that these parameters differ based on the conduit biomaterial. Although no consensus exists on the ideal conduit material for peripheral nerve repair, we have selected two commonly used animal-derived nerve conduits, SIS and CLC, for our study.<sup>17</sup> Our study evaluated total macrophages, M2 macrophages, foamy phagocytes, vasculature, collagen, and axon components in nerves repaired with two different nerve conduits (SIS and CLC).

## Materials and Methods

### Surgical procedures

This study used a total of 18 male Lewis rats (250–300 g). Rats were randomly assigned to be implanted with a SIS conduit (Axoguard Nerve Connector, Axogen Corporation,  $n = 9$ ) or CLC conduit (Neuragen Nerve Guide, Integra LifeSciences,  $n = 9$ , Fig. 1). Each rat

underwent a unilateral sciatic nerve transection approximately 5–7 mm distal to the sacroiliac ligament. Transected nerves were subsequently repaired with a nerve conduit, which was achieved by inserting approximately 2.5 mm of the proximal and distal nerve stumps into each end of a 10-mm conduit resulting in an approximately 5 mm gap between the nerve stumps. Conduits were secured with two single interrupted mattress stitches approximately 180° apart using a 9–0 nonabsorbable nylon suture on each nerve stump, ensuring that the coaptation had minimal tension. Each conduit was filled with sterile saline after implantation to remove air bubbles and maintain hydration. Surgical procedures and animal care conformed to the National Institutes of Health Guide for the Care and Use of Laboratory Animals. After 4 weeks, the implanted conduits, a cuff of surrounding soft tissue/muscle, and peripheral nerve were excised and processed for histological evaluation. The sciatic nerve from the contralateral leg, termed the contralateral healthy nerve, was also excised to evaluate the baseline Schwann cell population. The 4-week survival time point was selected to allow for Wallerian degeneration, macrophage differentiation, and axon regeneration across the nerve gap.<sup>9,18–20</sup>

### Histology

Contralateral healthy nerve samples were harvested approximately 3–5 mm distal to the sacroiliac ligament and extending 10 mm distal. Conduit samples were harvested to include the repair site, conduit, and approximately 3 mm of tissue proximal and distal to the end of the conduit. All samples were harvested to include the nerve and surrounding soft tissue. The distal nerve of each sample was marked with 8–0 nylon suture.

Implanted conduits and contralateral healthy nerve samples were placed in 10% neutral buffered formalin for at least 48 hours until embedding. Conduits and contralateral healthy nerve samples were embedded in paraffin blocks and transversely cut into 5  $\mu$ m sections. Conduit histology sections were collected at three levels: proximal nerve, mid-implant, and distal nerve (Fig. 2). Contralateral healthy nerve sections were collected at a similar location as the injured proximal stump level.

As shown in Table, contralateral healthy nerve sections were immunohistochemically stained to identify Schwann cells. Conduit histology sections were immunohistochemically stained to identify axon components, vascular components, Schwann cells, macrophages, foamy phagocytes, and M2 macrophages. Additional triple-staining using immunofluorescence was performed to visualize nuclei, M2 macrophages, and Schwann cells. Picrosirius red staining was used to evaluate collagen density.

Stained slides for the evaluation of axon components, vascular components, Schwann cells, macrophages, foamy phagocytes, and M2 macrophages were scanned using a Zeiss Axio Scan Z1 automated slide scanner (Carl-Zeiss) using a bright light source. Images of the entire sample cross-section were used for quantitative histological evaluation. Macrophage and foamy phagocytes were also imaged with an Olympus BX41 with a bright light source under magnification  $\times 400$ . These images provided representative images of macrophage and foamy phagocyte cell morphology but were not used for quantitative analysis. Slides stained for Schwann cells and M2 macrophages were imaged using an Olympus BX41 (Evident Olympus) with a fluorescent light source under various magnifications. Random fields were imaged at magnification  $\times 200$  for representative images of Schwann cells and M2 macrophages but were not used for quantitative analysis. Picrosirius red-stained collagen was imaged with an Olympus BX41 using a bright light source and a light polarizing filter. Images of random fields were collected at various magnifications, which were used for quantitative histological evaluation.

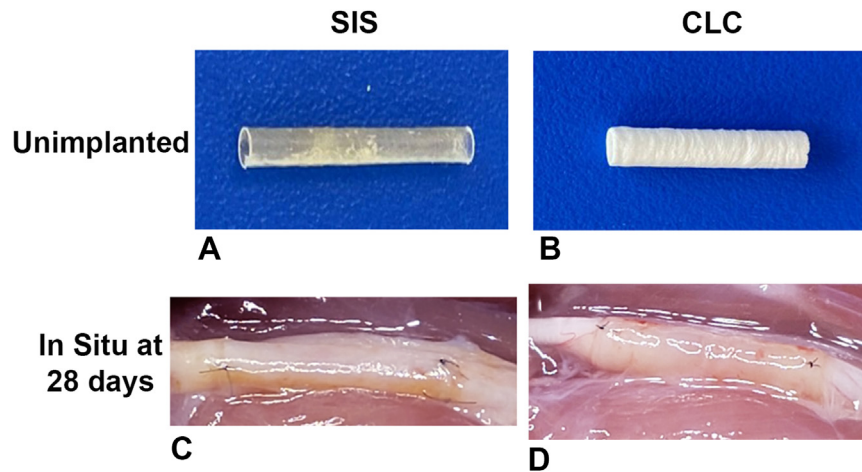


**Figure 1.** Representative images of **A** SIS before implant, **B** CLC before implant, **C** SIS immediately after implant, and **D** CLC immediately after implant.

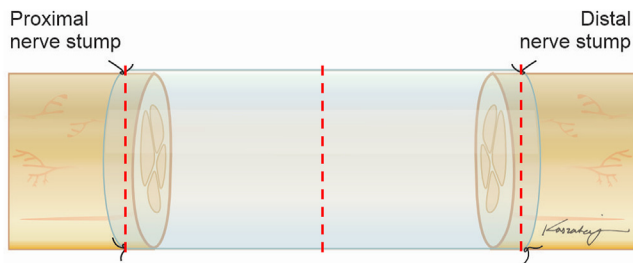


**Figure 2.** Representative image showing the approximate location of histological sections (red-dashed lines) in the conduit-repaired nerve. The proximal and distal nerve sections included the nerve stump and the surrounding nerve conduit. The mid-implant section included the regenerating nerve cable and the surrounding nerve conduit.

Macrophages and foamy phagocytes were identified by positive staining using CD68 antibody (Fig. 3A, B). Foamy phagocytes were differentiated from macrophages by using the following two criteria: (1) positive staining with CD68 and (2) an enlarged appearance with an apparent void, which is indicative of lipids from myelin and axonal debris that have been engulfed within the macrophages.<sup>14</sup> A notable presence of enlarged CD68-positive cells exists with an apparent void within the cells, which were categorized as foamy phagocytes (Fig. 3C, D).

Image analysis was performed using ImageJ (Fiji, National Institutes of Health). The numbers of M2 macrophages, macrophages, and Schwann cells were counted in the cross-sectional area of the nerve within the conduit. The nerve cross-section area was measured, and the results were recorded per 100,000  $\mu\text{m}^2$  of the nerve cable area, expressed as cell density. Foamy phagocytes and axon components were recorded using pixel density, where the number of pixels was determined in the cross-sectional area of the nerve within the conduit after image thresholding. The cross-sectional area of the nerve was measured, and the foamy phagocytes and axon component pixel counts were recorded as the number of pixels per 100,000  $\mu\text{m}^2$  of the nerve cable area. The quantification of foamy phagocytes was performed using pixel density, as a total count was confounded by the difficulty in defining individual cell borders. Immunofluorescence sections were used for representative images of M2 macrophages and Schwann cells. Slides stained with  $\alpha$ -smooth muscle actin were used to identify vascular components, which were counted in the cross-sectional area of the nerve within the conduit. The area of the

nerve was measured, and the results were recorded as the number of vessels per 100,000  $\mu\text{m}^2$ , expressed as vascular component density. Picrosirius red-stained slides were evaluated under polarized light to quantify the number of collagen pixels in the cross-sectional area of the nerve within the conduit. The area of the nerve was measured, and the results were recorded as collagen pixels per 100,000  $\mu\text{m}^2$ , expressed as collagen density.

#### Statistical analysis

Data from all animals were included in the statistical analyses. All data sets in this study were tested for a Gaussian (normal) distribution using a D'Agostino and Pearson test, and a  $P$  value of  $\leq .05$  was considered statistically significant. Schwann cell density, vascular component density, and axon component density were evaluated with two-way analysis of variance using conduit biomaterial (CLC vs SIS) and nerve histology location (proximal nerve, mid-implant, and distal nerve) as the main effects. Sidak post-tests were used when main effect differences were statistically significant. Schwann cell density of the contralateral healthy nerve was used as a reference and was not evaluated through statistical analysis. Collagen density, M2 macrophage density, and macrophage cell density were each evaluated using an unpaired  $t$  test with Welch's correction. This test was used to compare two groups (SIS vs CLC) with unequal variances. Foamy phagocyte cell density was evaluated using a Kolmogorov-Smirnov test, which was selected to compare the cumulative distribution between the two data sets (SIS vs CLC). A  $P$  value of  $\leq .05$  was considered statistically significant for all tests. Data are presented as means and 95% confidence intervals.

#### Results

Macrophage and M2 macrophage cell densities were significantly higher in the distal stump of nerves repaired with SIS versus CLC conduits,  $P = .002$  and  $P < .001$ , respectively (Fig. 4A, B). Foamy phagocyte cell density was significantly higher in the distal stump of CLC-repaired nerves compared with SIS-repaired nerves,  $P = .006$  (Fig. 5).

The Schwann cell density decreased from the proximal to the distal nerve in SIS-repaired nerves and CLC-repaired nerves (Fig. 6). Significantly higher Schwann cell density was observed in repairs with SIS versus CLC conduits at all histological levels,  $P < .001$  in the proximal nerve and mid-implant regions and  $P = .004$  in the distal

**Table**  
Location of Histological Staining and Imaging Techniques Within Nerve Explants

Explanted Sample	Target	Antibody	Proximal Nerve	Mid-Graft	Distal Nerve
Conduit (CLC and SIS) Contralateral Healthy Nerve	Schwann cells— immunohistochemistry	Primary: S100 (1:500 Abcam) Secondary: Goat anti-rabbit IgG HRP (1:2000, Abcam)	X	X	X
Conduit (CLC and SIS)	Triple Stain	Schwann cells— immunofluorescence	NA	NA	X
		M2 macrophages— immunofluorescence			
		Primary: CD163 (1:1000, Abcam) Secondary: Alexa Fluor 594 (1:200, Invitrogen) Vectashield mounting medium with DAPI (Vector Laboratories)			
	Axon components— neurofilament	Primary: Neurofilament (1:500, Abcam) Secondary: Goat anti-rabbit IgG HRP (1:1000, Abcam)	X	X	X
	Vascular components	Primary: $\alpha$ -smooth muscle actin (1:1000, Abcam) Secondary: Goat anti-rabbit IgG HRP (1:2000, Abcam)	X	X	X
	Collagen	Picrosirius red (Abcam)	NA	X	NA
	Macrophages and Foamy phagocytes	Primary: CD68 (1:500, Abcam) Secondary: Goat anti-rabbit IgG HRP (1:1000, Abcam)	NA	NA	X
	M2 macrophages	Primary: CD163 (1:100, Abcam) Secondary: Goat anti-rabbit IgG HRP (1:500, Abcam)	NA	NA	X

DAPI, diamidino-2-phenylindole; HRP, horseradish peroxidase.

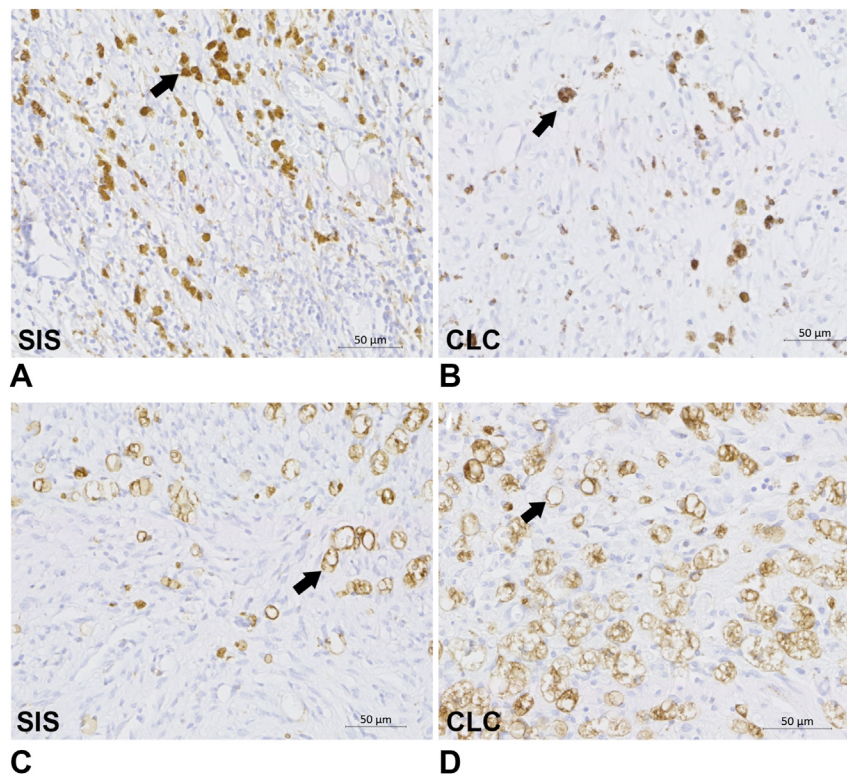


**Figure 3.** Representative photomicrographs of **A** CD68 immunohistochemistry of nerve repaired with SIS conduit showing macrophages, indicated by black arrows; **B** CD68 immunohistochemistry of nerve repaired with CLC conduit showing macrophages, indicated by black arrows; **C** CD68 immunohistochemistry of nerve repaired with SIS conduit showing foamy phagocytes, indicated by black arrows; and **D** CD68 immunohistochemistry of nerve repaired with CLC conduit showing foamy phagocytes, indicated by black arrows; magnification  $\times 400$ . Scale bar is 50  $\mu\text{m}$ .

nerve region. Additionally, the Schwann cell density of the contralateral healthy nerve was similar to the Schwann cell density nerves of repaired with CLC conduits in the proximal nerve region and SIS conduits in the mid-implant/distal nerve region.

Schwann cell (green) and M2 macrophage (red) expression was visually distinguishable in triple-stained immunofluorescence images. Less robust staining was noted in nerves repaired with CLC conduits (Fig. 7A-D) compared with nerves repaired with SIS

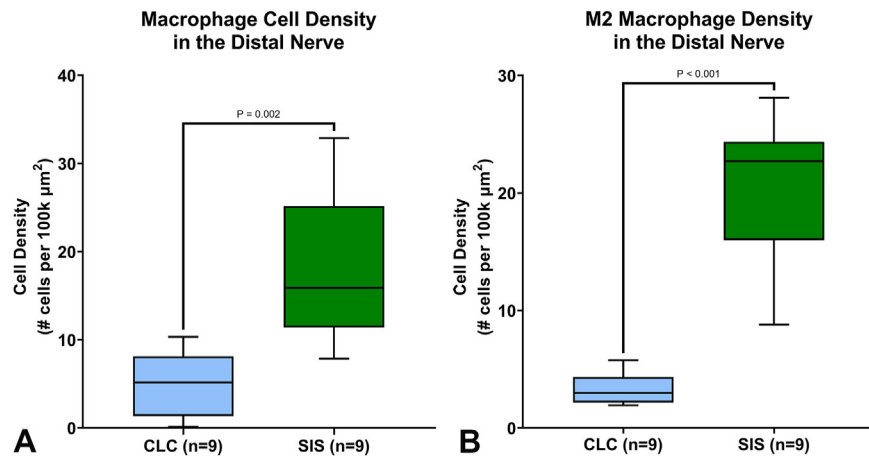


**Figure 4.** **A** Macrophage cell density was significantly higher in the distal stumps of SIS-repaired nerves versus CLC-repaired nerves,  $P = .002$ . **B** M2 macrophage density was significantly higher in the distal nerve regions of SIS-repaired nerves versus CLC-repaired nerves,  $P < .001$ .

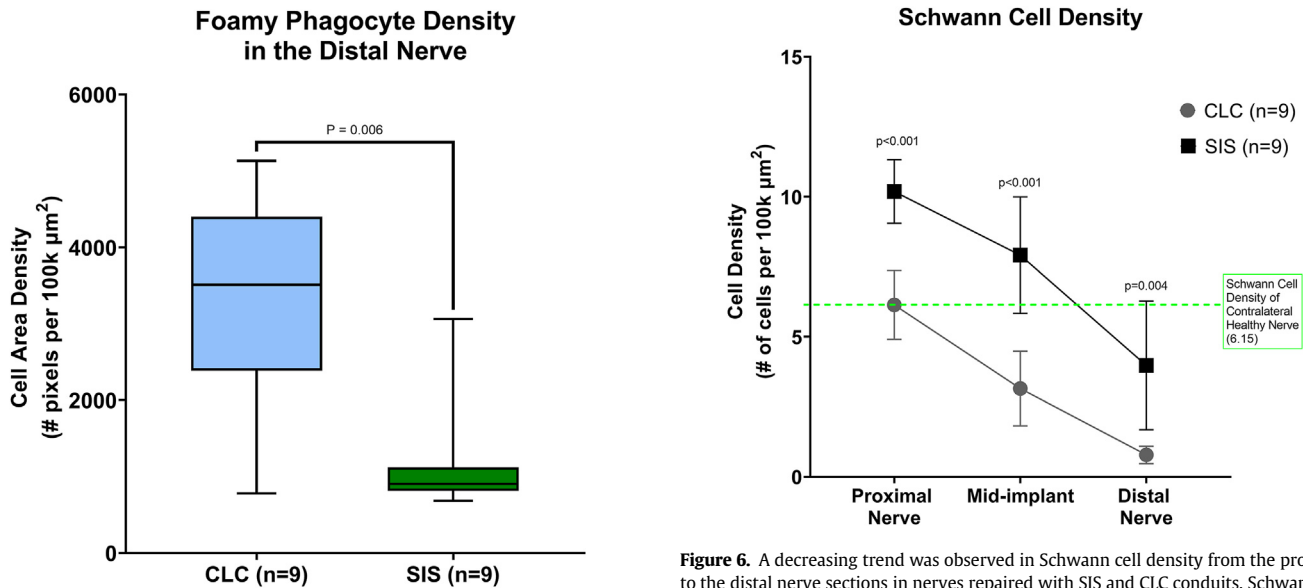


**Figure 5.** Foamy phagocyte cell density was significantly higher in the distal stumps of nerves repaired with CLC versus those repaired with SIS,  $P = .006$ .

conduits (Fig. 7E-H), which supports the quantitative assessments in Figures 4B and 6.

No change was observed in vascular component density from the proximal nerve through the distal nerve within each group. The density of the vascular components in the proximal nerve, mid-implant, and distal nerve was significantly higher in nerves repaired with SIS conduits compared with nerves repaired with CLC conduits ( $P = .01$  in the proximal nerve region and  $P < .001$  in the mid-implant and distal nerve regions, Fig. 8).

No significant differences were found in the axon component density, quantified by neurofilament density, in the proximal nerve and distal nerve regions between nerves repaired with SIS conduits versus nerves repaired with CLC conduits,  $P = .21$  and  $P > .99$ , respectively. In the mid-implant region, the axon component density was significantly higher in nerves repaired with SIS conduits compared with nerves repaired with CLC conduits ( $P = .006$ , Fig. 9).

Overall, a low density of collagen was noted in both groups, but significantly higher collagen density was observed in the mid-

**Figure 6.** A decreasing trend was observed in Schwann cell density from the proximal to the distal nerve sections in nerves repaired with SIS and CLC conduits. Schwann cell density was significantly higher in nerves repaired with SIS versus CLC conduits at all histological levels,  $P < .001$  in the proximal nerve and mid-implant regions and  $P = .004$  in the distal nerve region. The contralateral healthy nerve Schwann cell density was higher than nerves repaired with CLC conduits in the mid-implant and distal nerve regions but similar in the proximal nerve region. The contralateral healthy nerve Schwann cell density was lower than nerves repaired with SIS conduits in the proximal nerve and mid-implant regions but higher than nerves repaired with SIS in distal nerve region.

implant intraneural space of nerves repaired with CLC conduits versus nerves repaired with SIS conduits,  $P = .01$  (Fig. 10).

## Discussion

A previous in vivo nerve transection study showed a greater M2:M1 response, more revascularization, more fibroblast ingrowth, and more lymphocytes through the mid-implant wall of SIS nerve conduits versus CLC nerve conduits, and more regenerated nerve cable density of the mid-implant region of the nerve within SIS-repaired nerves versus CLC-repaired nerves at 4 weeks post-transection.<sup>16</sup> We expanded on these findings and quantified macrophages, M2 macrophages, foamy phagocytes, Schwann cells, axon components, vascular components, and collagen density to

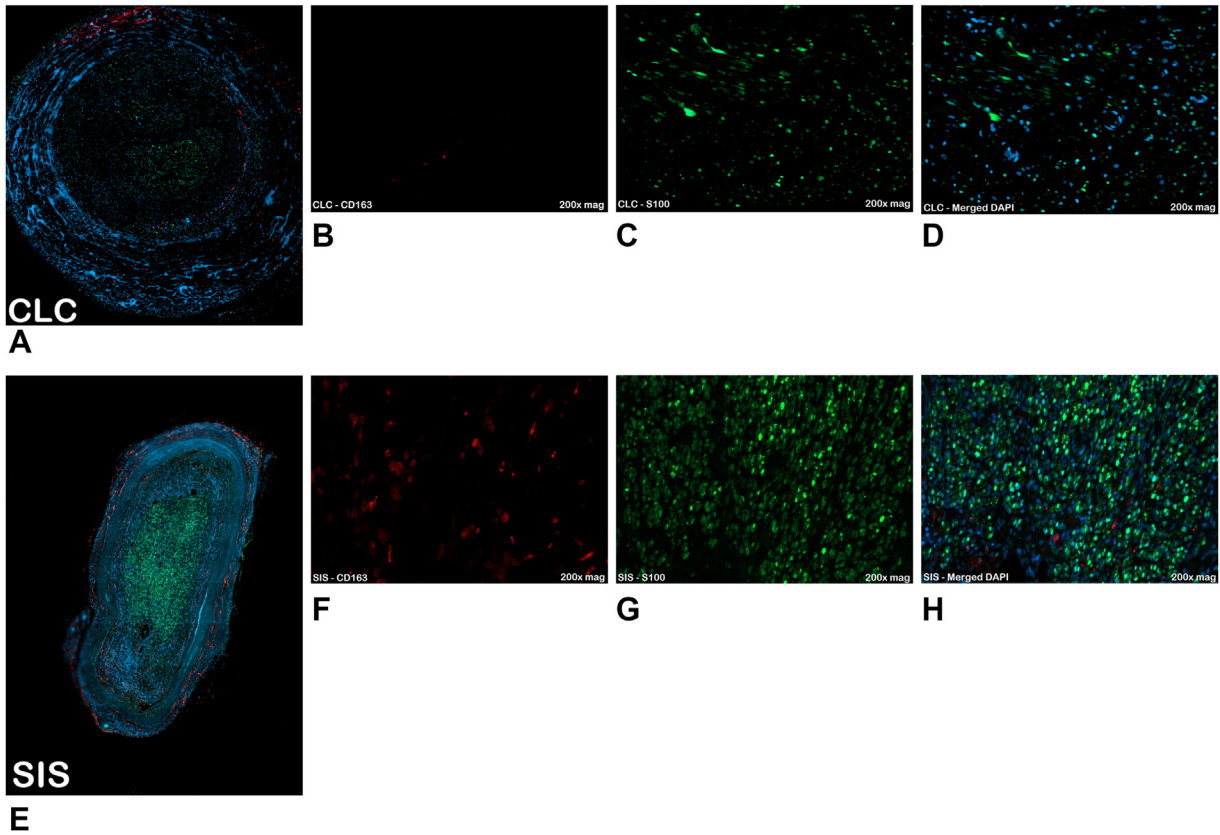


**Figure 7.** Representative photomicrographs of triple immunofluorescence staining for M2 macrophages (red), Schwann cells (green), and cell nuclei (blue) within the distal nerve region. There appeared to be fewer M2 macrophages and Schwann cells in A–D nerves repaired with CLC conduits than in E–H nerves repaired with SIS conduits.

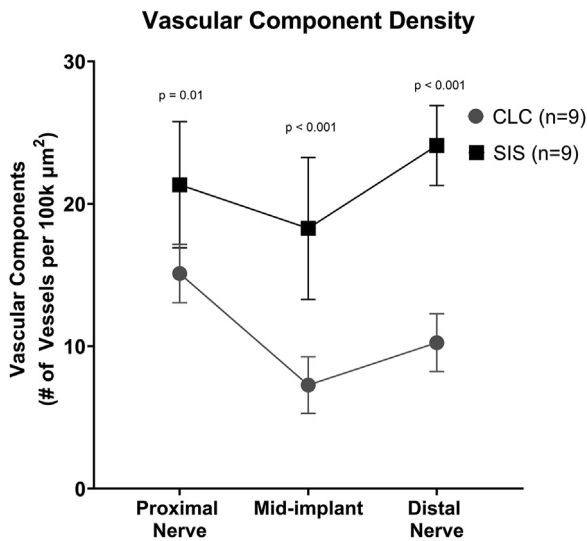


**Figure 8.** The vascular component density of nerves repaired with SIS conduits was significantly higher than nerves repaired with CLC conduits at all histology levels,  $P = .01$  at the proximal nerve region,  $P < .001$  at the mid-implant and distal nerve regions.

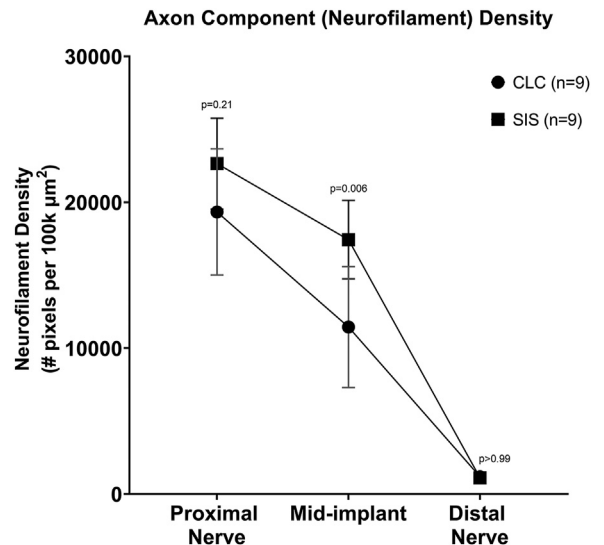


**Figure 9.** Density of axon components, measured by neurofilament staining, showed a decreasing trend in density in both groups. A significantly higher density was observed in nerves repaired with SIS conduits versus CLC conduits in the mid-implant region,  $P = .006$ . No significant differences were observed in nerves repaired with SIS conduits versus nerves repaired with CLC conduits in the proximal nerve and distal nerve regions,  $P = .21$  and  $P > .99$ , respectively.

evaluate the progression of Wallerian degeneration and nerve regeneration. We investigated the total macrophage and M2 macrophage populations in the distal nerve, as macrophage differentiation has been reported to influence peripheral nerve regeneration more than the number of total macrophages.<sup>11</sup> Modulating the initial macrophage phenotype has been shown to influence the biochemical cascade of the inflammatory process,

resulting in either a proinflammatory (higher M1) or anti-inflammatory (higher M2) response.<sup>11</sup> This early influence in macrophage modulation lessens the need to modulate the process downstream after a peripheral nerve injury.<sup>11</sup> The transformation

### Mid-implant Collagen Density Within the Nerve Evaluated by Polarization of Picro-sirius Red

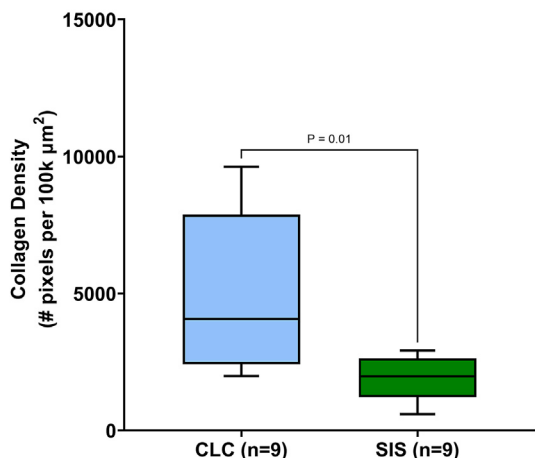


**Figure 10.** Collagen density in the mid-implant intraneural space was significantly higher in nerves repaired with CLC conduits versus nerves repaired with SIS conduits,  $P = .01$ .

of macrophages to foamy phagocytes has been shown to play a role in Wallerian degeneration, as these cells remove regeneration-limiting components, myelin, and axonal debris.<sup>8,13</sup> We also investigated collagen density and vascular components, which provides valuable information regarding tissue remodeling, as scarred nerve exhibits more collagen and less vasculature.<sup>21</sup>

We found significantly higher populations of total macrophages, driven by a similar increase in M2 macrophages, in the distal nerve region of nerves repaired with SIS conduits versus nerves repaired with CLC conduits. High M2 macrophage levels are associated with inflammation resolution and promoting healing.<sup>12</sup> The nerves repaired with CLC conduits contained a higher population of foamy phagocytes in the distal nerve region compared with nerves repaired with SIS conduits. A higher population of foamy phagocytes may indicate an ongoing Wallerian degeneration process in the nerves repaired with CLC conduits.

The vascular component density and Schwann cell density of nerves repaired with SIS conduits were significantly higher than that in nerves repaired with CLC conduits. This vascular network is critical to cell survival and provides a pathway for the migration of Schwann cells,<sup>22</sup> which supports the vascular component density and Schwann cell density data reported in our study. Mokarram et al<sup>11</sup> found that M2 macrophages increased Schwann cell migration two-fold compared with cell migration induced by M1 macrophages. It is possible that the higher density of M2 macrophages may have affected the Schwann cell density, as Schwann cells are critical to both Wallerian degeneration and nerve regeneration.<sup>23</sup>

A higher axon component density was found in the mid-implant region of nerves repaired with SIS conduits versus nerves repaired with CLC conduits; however, no differences were observed in the proximal nerve and distal nerve regions. Picrosirius red staining showed a significantly lower concentration of collagen in the intraneural space of the mid-implant region of nerves repaired with SIS conduits compared with nerves repaired with CLC conduits. The presence of more axon component density with less collagen density in the mid-implant nerve region of nerves repaired with SIS versus nerves repaired with CLC conduits may indicate better axonal regeneration and less collagenous or scar tissue formation in the nerves repaired with SIS conduits. Similar results were noted by Hanwright et al<sup>24</sup> who found that extracellular matrix nerve wraps decreased intraneural collagen deposition,

indicating less scar formation. Although the nerves of both groups were surrounded by a nerve conduit, the differences between the SIS-repaired nerves and the CLC-repaired nerves may be attributable to differences in the conduit material.

In summary, these findings demonstrated that the nerves repaired with SIS conduits exhibited more total macrophages, specifically due to higher levels of M2 macrophages. These M2 macrophages are a phenotype associated with resolution of inflammation and conclusion of healing. The foamy phagocytes were higher in nerves repaired with CLC conduits versus nerves repaired with SIS conduits, which suggests a slower resolution of Wallerian degeneration in nerves repaired with CLC conduits. However, without additional time points, the resolution of this process cannot be definitive. Our study showed more vascular components and Schwann cell density throughout the nerve in repairs with SIS conduits compared with nerves repaired with CLC conduits, which is critically important for organized peripheral nerve regeneration. Axon component density in the mid-implant region of SIS-repaired nerves was significantly higher than CLC-repaired nerves. No significant differences were noted in the axon component density of the distal nerve region; however, this may be due to the early time point evaluated in this study, where axons have not yet reached the distal nerve region. Nerves repaired with SIS conduits showed less collagen deposition and higher axon component density in the mid-implant region of nerve cross-sections. These findings suggest better nerve regeneration with less scar tissue formation in the nerves repaired with SIS conduits compared with nerves repaired with CLC conduits. A permissive growth environment is the result of effective myelin and axonal debris phagocytosis by invading macrophages and resident Schwann cells, as well as the support of appropriate extracellular matrix deposition and axon regeneration.<sup>25</sup>

The data presented in this study indicate meaningful differences, particularly in the mid-implant regions of the nerves repaired with SIS conduits. This study was limited in collected data because nerve function testing was not performed, and the time point for evaluation was acute at 4 weeks. Although functional testing would be beneficial to this evaluation, the limited 4-week in-life timeline precluded adequate time for the evaluation of nerve function. This study also did not capture any histological evaluations past the 4-week time point. In-life time points after 4 weeks may provide data showing the resolution of Wallerian degeneration in the nerves repaired with CLC conduits and more complete nerve regeneration, especially in the distal nerve region of both groups. Future studies should consider including additional in-life time points at longer durations, which would allow for adequate evaluation of functional testing and additional histological characterization. Despite these limitations, this study provides a valuable characterization of the quality of regeneration after repair with two commonly used nerve conduits and serves to expand on the current literature.

### Acknowledgments

The authors would like to thank Anne Engemann for her contributions in planning and reviewing this research study.

### References

1. Ducic I, Safa B, Devinney E. Refinements of nerve repair with connector-assisted coaptation. *Microsurgery*. 2017;37(3):256–263.
2. Devices@FDA - JXI Code. Date. Accessed April 21, 2022. [https://www.accessdata.fda.gov/scripts/cdrh/devicesatfda/index.cfm?start\\_search=1&q=Slh&approval\\_date\\_from=&approval\\_date\\_to=&sort=approvaldatedesc&pagenum=10](https://www.accessdata.fda.gov/scripts/cdrh/devicesatfda/index.cfm?start_search=1&q=Slh&approval_date_from=&approval_date_to=&sort=approvaldatedesc&pagenum=10)
3. Kehoe S, Zhang XF, Boyd D. FDA approved guidance conduits and wraps for peripheral nerve injury: a review of materials and efficacy. *Injury*. 2012;43(5):553–572.

4. Yan Y, Yao R, Zhao J, et al. Implantable nerve guidance conduits: material combinations, multi-functional strategies and advanced engineering innovations. *Bioact Mater*. 2022;11:57–76.
5. Gaudet AD, Popovich PG, Ramer MS. Wallerian degeneration: gaining perspective on inflammatory events after peripheral nerve injury. *J Neuroinflammation*. 2011;8(1):110.
6. Burnett MG, Zager EL. Pathophysiology of peripheral nerve injury: a brief review. *Neurosurg Focus*. 2004;16(5):1–7.
7. Brück W. The role of macrophages in Wallerian degeneration. *Brain Pathol*. 1997;7(2):741–752.
8. Chen P, Piao X, Bonaldo P. Role of macrophages in Wallerian degeneration and axonal regeneration after peripheral nerve injury. *Acta Neuropathol*. 2015;130(5):605–618.
9. Rotshenker S. Wallerian degeneration: the innate-immune response to traumatic nerve injury. *J Neuroinflammation*. 2011;8(1):109.
10. Stoll G, Griffin JW, Li CY, et al. Wallerian degeneration in the peripheral nervous system: participation of both Schwann cells and macrophages in myelin degradation. *J Neurocytol*. 1989;18(5):671–683.
11. Mokarram N, Merchant A, Mukhatyar V, et al. Effect of modulating macrophage phenotype on peripheral nerve repair. *Biomaterials*. 2012;33(34):8793–8801.
12. Badylak SF, Valentin JE, Ravindra AK, et al. Macrophage phenotype as a determinant of biologic scaffold remodeling. *Tissue Eng Part A*. 2008;14(11):1835–1842.
13. Griffin JW, George R, Lobato C, et al. Macrophage responses and myelin clearance during Wallerian degeneration: relevance to immune-mediated demyelination. *J Neuroimmunol*. 1992;40(2–3):153–165.
14. Grajchen E, Hendriks JJA, Bogie JFJ. The physiology of foamy phagocytes in multiple sclerosis. *Acta Neuropathol Commun*. 2018;6(1):124.
15. Perry VH, Brown MC, Gordon S. The macrophage response to central and peripheral nerve injury. A possible role for macrophages in regeneration. *J Exp Med*. 1987;165(4):1218–1223.
16. Zhukauskas R, Fischer DN, Deister C, et al. A comparative study of porcine small intestine submucosa and cross-linked bovine type I collagen as a nerve conduit. *J Hand Surg Glob Online*. 2021;3(5):282–288.
17. Beris A, Gkiatas I, Gelalis I, et al. Current concepts in peripheral nerve surgery. *Eur J Orthop Surg Traumatol*. 2019;29(2):263–269.
18. Min Q, Parkinson DB, Dun XP. Migrating Schwann cells direct axon regeneration within the peripheral nerve bridge. *Glia*. 2021;69(2):235–254.
19. Sunderland IR, Brenner MJ, Singham J, et al. Effect of tension on nerve regeneration in rat sciatic nerve transection model. *Ann Plast Surg*. 2004;53(4):382–387.
20. Otake K, Toriumi T, Ito T, et al. Recovery of sensory function after the implantation of oriented-collagen tube into the resected rat sciatic nerve. *Regen Ther*. 2020;14:48–58.
21. Deng H, Li-Tsang CWP. Measurement of vascularity in the scar: a systematic review. *Burns*. 2019;45(6):1253–1265.
22. Fornasari BE, Zen F, Nato G, et al. Blood vessels: the pathway used by Schwann cells to colonize nerve conduits. *Int J Mol Sci*. 2022;23(4):2254.
23. Negro S, Pirazzini M, Rigoni M. Models and methods to study Schwann cells. *J Anat*. 2022.
24. Hanwright PJ, Rath JB, von Guionneau N, et al. The effects of a porcine extracellular matrix nerve wrap as an adjunct to primary epineurial repair. *J Hand Surg Am*. 2021;46(9):813.e1–813.e8.
25. Fu SY, Gordon T. The cellular and molecular basis of peripheral nerve regeneration. *Mol Neurobiol*. 1997;14(1–2):67–116.